Observation of thermoacoustic chaoticoscillations in a looped tube

doi: 10.1063/1.5066363

Observation of thermoacoustic chaotic oscillations in a looped tube

Cite as: Chaos **29**, 093108 (2019); https://doi.org/10.1063/1.5066363
Submitted: 15 October 2018 . Accepted: 09 August 2019 . Published Online: 09 September 2019

Rémi Delage, Yusuke Takayama, Hiroaki Hyodo, and Tetsushi Biwa

Observation of thermoacoustic chaotic oscillations in a looped tube

Cite as: Chaos **29**, 093108 (2019); doi: 10.1063/1.5066363
Submitted: 15 October 2018 · Accepted: 9 August 2019 ·
Published Online: 9 September 2019

Rémi Delage, Yusuke Takayama, Hiroaki Hyodo, and Tetsushi Biwa

AFFILIATIONS

Department of Mechanical Engineering, Tohoku University, Sendai 980-8579, Japan

ABSTRACT

This study presents experimental observations of chaotic thermoacoustic oscillations induced in a looped tube with respect to both temporal and spatial dimensions and compares them with those in a resonance tube system. The wave propagation directions observed in thermoacoustic systems showing periodic behaviors are confirmed in the chaotic case, from cold to hot sides in the stack in a looped system, and with reflections at the ends of a resonance tube system. Although both systems are similar in their route to chaos and correlation dimensions of the chaotic attractor, a recurrence visualization method reveals differences in the distribution of temporal patterns resulting from the mode competition between the natural frequencies of the systems.

Thermoacoustics is an emerging field of study in which understanding of theoretical linear stability analysis is already well established.[1,2] However, there is still a lack of knowledge on nonlinear phenomena occurring at high amplitudes, such as chaotic oscillations. The first step in the understanding of such phenomena requires complete experimental observations. Spatio-temporal observations have already been performed for periodic oscillations with shockwaves in both straight and loop thermoacoustic systems, verifying the standing wave and traveling wave profiles. The current study aims to understand thermoacoustic chaotic oscillations, and, to some extent, chaotic behaviors in dissipative fluid systems, by reporting the spatio-temporal measurement in both straight and looped systems.

I. INTRODUCTION

Thermoacoustic oscillators are a class of dissipative fluid systems that show self-sustained acoustic oscillations when a gas column confined in a tube is locally heated or cooled until the temperature ratio between the hot and cold parts becomes sufficiently high. Reflecting the tube geometry, two types of thermoacoustic oscillations are generated: one is a standing wave mode oscillation in a resonance tube[3,4] with open and/or closed ends, and the other is a traveling wave mode oscillation in a looped tube.[5–7] In both oscillation modes, the generated acoustic gas oscillations are almost sinusoidal functions of time having natural frequencies when the temperature gradient is just above the critical one, but the waveform distorts at elevated temperature ratios.

It has been observed both experimentally and numerically that a high temperature ratio leads to a periodic pressure wave with shock fronts moving back and forth in the resonance tube[8,9] and traveling in one direction in the looped tube.[9,10] In some experimental systems, even chaotic oscillations are generated owing to higher temperature ratios.[11,15] However, these thermoacoustic chaotic oscillations have only been observed in resonance tubes so far. Furthermore, measurement of the spatio-temporal evolution of chaotic oscillations has been a difficult experimental task because of the extreme temperature conditions generated by using liquid helium[11] or combustion reactions of air-fuel mixtures.[15]

From a theoretical point of view, the thermoacoustic system has been discussed as a stability problem of hydrodynamics.[2,3,16] Although the theoretical results of the linear stability analysis are validated by various experiments,[6,17–20] it is still challenging to make an elaborate nonlinear analysis that can describe thermoacoustic chaotic oscillations based on the fundamental equations of hydrodynamics, as demonstrated in Rayleigh-Bénard convection systems.

This study experimentally reports the thermoacoustic chaotic oscillations in a looped tube. We have recently succeeded in generating chaotic oscillations in a resonance tube by making the system dissonant,[21] although the major part of the tube was maintained at room temperature. In this paper, we apply the same technique to a looped tube thermoacoustic system to excite chaotic acoustic gas oscillations. A spatio-temporal measurement of pressure fluctuations

reveals differences between the fast and slow dynamical patterns of chaotic oscillations in the resonance and looped tubes.

II. EXPERIMENTS

A. Looped tube thermoacoustic system

Figure 1(a) shows the looped tube thermoacoustic system, which was made of straight acrylic cylindrical tubes with a 48 mm inner diameter and a pair of 180° bend sections, each of which was made of two 90° steel elbows with the same diameter as the straight tubes. The loop had an average length of $L = 4.16$ m, was filled with air at ambient temperature and pressure, and contained a stack sandwiched by cold and hot heat exchangers with temperatures of T_C and T_H, respectively. The stack was made of a 20 mm long cylindrical ceramic honeycomb catalyst which had square pores with a side length of 0.68 mm. Temperatures T_C and T_H were measured at the cold and hot sides of the stack using thermocouples inserted into the pipe. The heat exchangers were made of brass strips with a thickness of 0.5 mm and 1.0 mm apart from each other. The hot heat exchanger was heated by feeding electrical current to a sheathed wire heater wound around it, whereas the cold heat exchanger was cooled by circulating water at an ambient temperature of 293 K. A cooling water pipe was also wound around the 48 mm diameter tube and separated from the hot heat exchanger by 35 mm. Thus, the looped tube was mostly maintained at room temperature during the experiments.

This system started to excite acoustic gas oscillations with a frequency of $f_2 = 164$ Hz when the temperature ratio T_H/T_C was increased to 1.90. The oscillation mode corresponds to the second longitudinal acoustic mode of the looped tube as f_2 was close to $2a/L$, where a denotes the sound speed and L is the average length of the loop. The acoustic pressure, monitored by using a small pressure transducer located at $x = 2.7$ m, was almost sinusoidal; x represents the axial coordinate taken along the tube axis going from cold to hot in the stack, with $x = 0$ at the center of the stack. With an elevated temperature ratio of $T_H/T_C = 2.30$, the temporal variation of the pressure became noticeably distorted because of the excited oscillations of the higher harmonics. At $T_H/T_C = 2.64$, the pressure oscillations were confirmed to evolve into periodic shock waves with discontinuous wavefronts. Further increase of T_H/T_C resulted in an increase of pressure discontinuity.

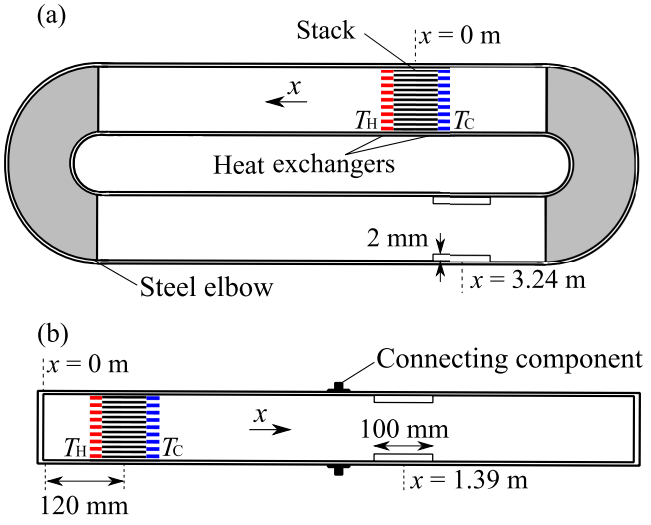

FIG. 1. Schematic illustration of thermoacoustic systems: (a) looped tube and (b) resonance tube.

Observations of thermoacoustic shock waves have been reported in previous experimental and numerical studies on thermoacoustic systems made of a straight resonance tube.[8,9] We have experienced that the local contraction of the tube diameter is able to turn the periodic shock waves into chaotic oscillations.[21] Breaking the system's symmetry with this small pipe increased the number of modes with incommensurate frequencies, excitable within the reachable range of temperature ratios. With the increasing number of incommensurate frequencies, an overall locking phenomenon was less likely to prevail, and the nonlinear interactions eventually caused the system to become chaotic. Therefore, we inserted a 2 mm thick and 100 mm long pipe into the looped tube, to achieve the same impact on the traveling thermoacoustic oscillations.

In the looped tube system installed with the small pipe, the chaotic oscillations were explored by changing the position of the pipe with a step of 0.1 m in a range of $1.74\,\text{m} < x < 3.34\,\text{m}$, at a constant heating power of 450 W. This was the maximum power applicable by the present heater wire. We found two areas, $3.14\,\text{m} < x < 3.34\,\text{m}$ and $2.44\,\text{m} < x < 2.54\,\text{m}$, in which the chaotic oscillations were confirmed, and decided to put the small pipe at $x = 3.24$ m in the middle of the wider area.

When installed with the small pipe at that position, the system started to oscillate with $f_3 = 244$ Hz in the third acoustic mode at $T_H/T_C = 1.84$; it entered the quasiperiodic state with incommensurate frequencies f_3 and $f_1 = 80.4$ Hz with $T_H/T_C > 1.97$ and was finally found to reach the chaotic state characterized with broad peaks at base frequencies f_1, f_2, and f_3 in the amplitude spectrum when $T_H/T_C = 2.19$.

Figure 2(a) shows a chaotic pressure oscillation in the looped tube measured at $x = 73$ mm. This measurement is a part of spatio-temporal observation using many pressure transducers. The measurement method is described below. Slow dynamics with aperiodic beating was observed, as well as fast dynamics associated with the base frequencies f_1 and f_3. In the magnified view (a1) at times $t = 5.6$ s, one can see the third mode oscillations slightly modulated by the first mode oscillations, whereas, in the magnified view (a2) at time $t = 7.6$ s, the first mode oscillations are more visible, as one can see from the time intervals $\tau_3 = 1/f_3$ and $\tau_1 = 1/f_1$.

To quantify the chaotic behavior, we evaluated the correlation dimension ν defined as

$$\nu = \lim_{r\to 0} \frac{\log C(r)}{\log r}, \tag{1}$$

where C is the correlation integral,

$$C(r) = \frac{1}{N^2} \sum_{i,j=1}^{N} \Theta\left(r - \left\|\vec{z}_i - \vec{z}_j\right\|\right), \qquad i \neq j, \tag{2}$$

and N is the number of considered points $\vec{z}_i$ in the phase space (here built using the embedding method[22]), r is the arbitrary distance,

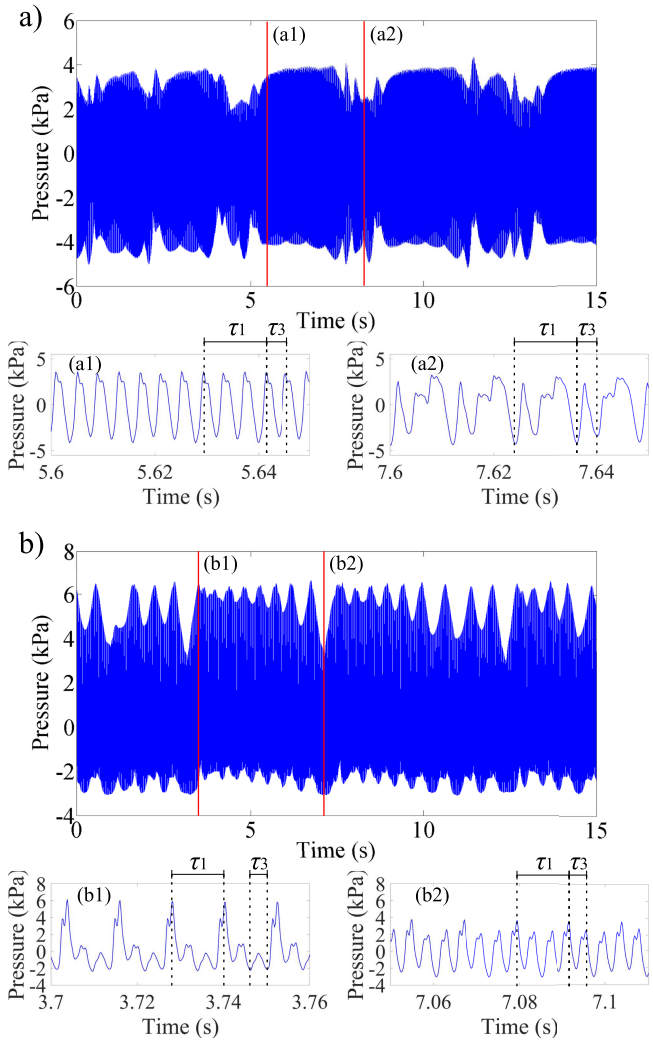

FIG. 2. Chaotic time series obtained from (a) the loop system and (b) the resonant system over a long time scale. Short-time behaviors are shown in (a1), (a2), (b1), and (b2) with time indications for the first and third mode oscillation periods $\tau_1 = 1/f_1$ and $\tau_3 = 1/f_3$.

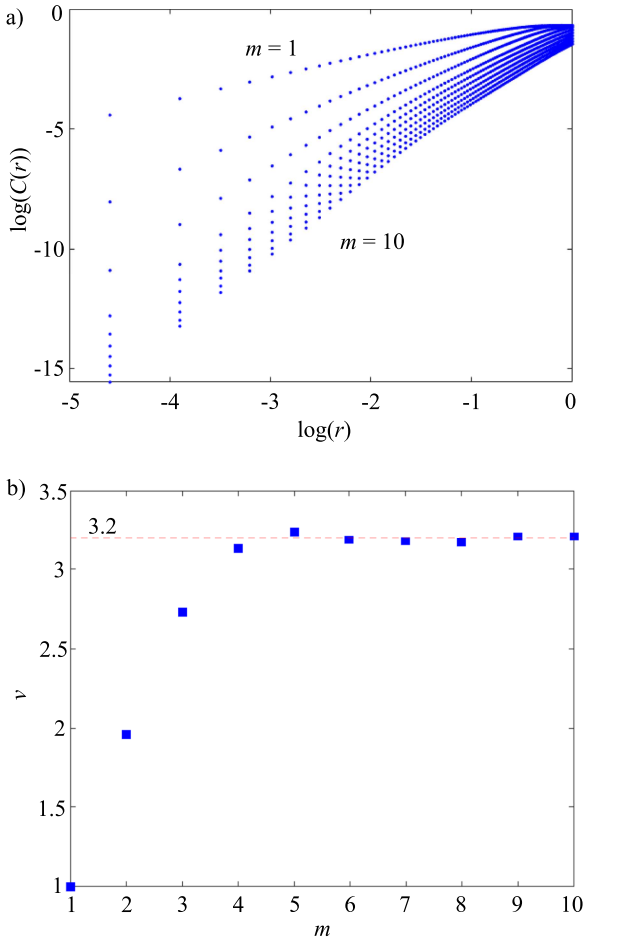

FIG. 3. (a) Log-log graph of the correlation integral for embedding dimensions $m = 1$ to 10 calculated from the normalized time series of Fig. 2(a). (b) Correlation dimension ν estimated from the slope of (a) between $\log(r) = -3.5$ to -2.5 using the least square fitting method.

and Θ is the heaviside function.[11] In the calculation, we used 60 000 points of pressure signals, low-pass filtered with 1 kHz, and sampled at 2.5 kHz, as shown in Fig. 2(a). The calculation up to 10 dimensions indicated that ν was equal to 3.2 ± 0.1. Figures 3(a) and 3(b) show the convergence of ν as the phase space dimension m increases. The slope of the correlation integral on a logarithmic scale reaches 3.2 above $m = 4$.

In order to confirm that the noninteger correlation dimension does not result from stochastic noise in our time series, we tested the data using pseudoperiodic surrogate testing introduced by Small *et al.*[12] This testing method has been used to confirm the existence of nonperiodic intercycle dynamics in thermoacoustic systems.[13,14] After generating 30 surrogates using $m = 4$ embedding from the chaotic time series shown in Fig. 2(a), we calculated the correlation dimension for all surrogates and the original data. The results are shown in Fig. 4, in which one can see a clear difference from the correlation dimensions of the surrogates, so the null hypothesis of periodic orbit with uncorrelated noise is rejected.

B. Resonance tube thermoacoustic system

In order to make a comparison with the looped tube system, we investigated a resonance tube thermoacoustic system, as shown in Fig. 1(b). It was made of 48 mm diameter cylindrical tubes with a total length of $L_R = 2.10$ m and was installed with a stack and a pair of heat exchangers in the same way as the looped tube. The resonance tube length was set so that the natural frequencies defined by $f_n \approx na/(2L_R)$ $(n = 1, 2, 3,\ldots)$ were close to those in the looped system defined by $f_n \approx na/L$. The stack pore size was the same as that used in the looped tube. Again, a 2 mm thick walled cylindrical pipe

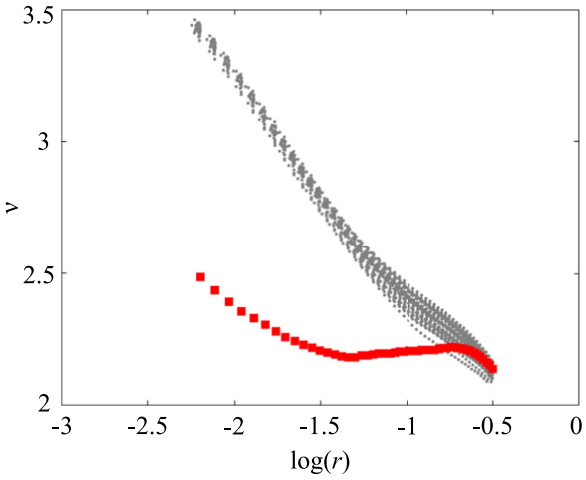

FIG. 4. Correlation dimensions ν with $m = 4$ of the original data (red squares) and 30 pseudoperiodic surrogates (grey dots) for the time series shown in Fig. 2(a) after normalization. The correlation dimension differs clearly from the surrogates.

with a length of 100 mm was placed at $x = 1.39$ m to prevent the shock wave formation. Here, x is measured from the hot end to the opposite end, with $x = 0$ m at the closed end near the hot part.

When T_H was elevated while keeping T_C at the ambient temperature, the resonance tube thermoacoustic system started to generate acoustic gas oscillations with the third natural frequency $f_3 = 250.2$ Hz at $T_H/T_C = 1.91$ and entered the chaotic regime at $T_H/T_C = 2.40$ via quasiperiodic oscillation states of f_1 and f_3 modes. The amplitude spectrum consisted of major broad peaks around the natural frequencies f_1, f_2, and f_3, and the correlation dimension of the chaotic attractor was found to be 3.2 ± 0.1, from the pressure oscillations measured at the end of the resonance tube with $T_H/T_C = 2.40$. Figure 2(b) shows a typical time series obtained in the resonant system with $T_H/T_C = 2.74$. As in the looped system, the fast dynamics alternate between mostly third mode oscillation phases and phases where first mode oscillations are visible, as can be seen from the magnified views in (b1) and (b2). Again, the chaotic behavior appeared in the aperiodic slow beating.

The correlation dimension of 3.2 ± 0.1 in the resonance tube was equal to that estimated in the looped tube. Similar correlation dimensions were obtained at different measurement positions x in both systems. Therefore, it was found that the point measurement of the pressure did not detect a significant difference between thermoacoustic chaotic oscillations in the looped tube and in the resonance tube. Furthermore, we tested the chaotic time series obtained in the resonant systems using the pseudoperiodic surrogates data testing which also led to the rejection of the null hypothesis of a periodic orbit with stochastic noise.

C. Spatio-temporal measurement method

To observe the spatial structure of thermoacoustic chaotic oscillations, we conducted simultaneous measurements of pressure oscillations at different axial positions. Several pressure transducers were placed on the tube walls via small ducts of 2 mm internal diameter and 10 mm length. In total, 52 pressure transducers were placed with an axial spacing of 65 mm in the looped tube and 37 pressure transducers with a spacing of 50 mm in the resonance tube. The transducers were not located in the 90° elbow regions in the looped tube and in the short section at the middle of the resonance tube, where two 48 mm tubes were connected by a tube fitting.

The pressure signals, after amplification by DC amplifiers and low-pass filtered at 1 kHz, were sampled by a multichannel A/D converter at a sampling frequency of 5 kHz for a time interval of 15 s. During the measurements, the temperature ratio was kept at $T_H/T_C = 2.74 \pm 0.01$ to warrant chaotic oscillations both in the looped tube and in the resonance tube thermoacoustic systems.

III. RESULTS AND DISCUSSION

The results for the looped tube and the straight tube are shown in Figs. 5 and 6, where the horizontal and vertical axes represent the

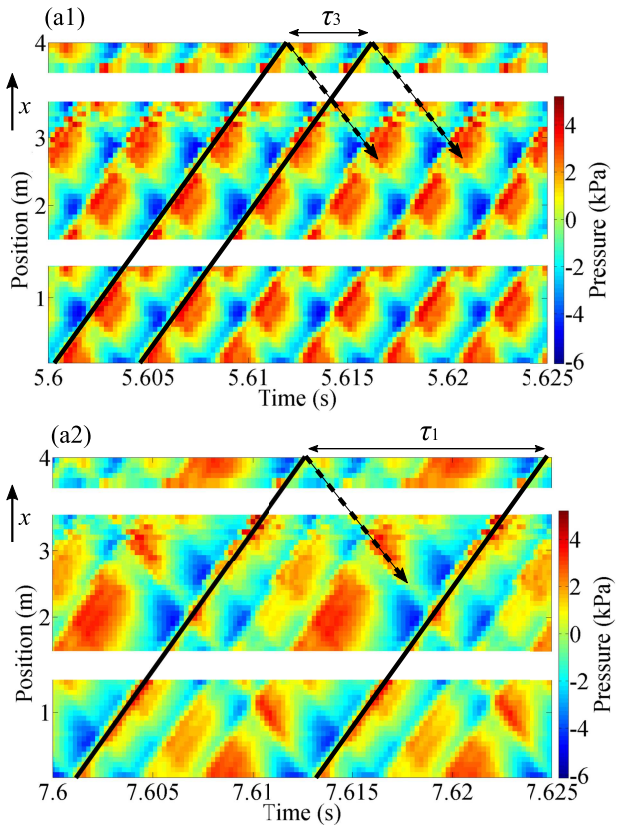

FIG. 5. Spatio-temporal chaotic data obtained from the loop system at times (a1) and (a2) in Fig. 2(a). Examples of pressure waves propagation in the positive x direction are indicated by solid lines separated by typical time intervals $\tau_1 = 1/f_1$ and $\tau_3 = 1/f_3$. The less intense reflected waves propagating in the negative x direction are indicated by dashed lines. See Multimedia view for a stroboscopic animation corresponding to the first 10 s slow down to 1/3 of the actual speed. Multimedia view: https://doi.org/10.1063/1.5066363.1

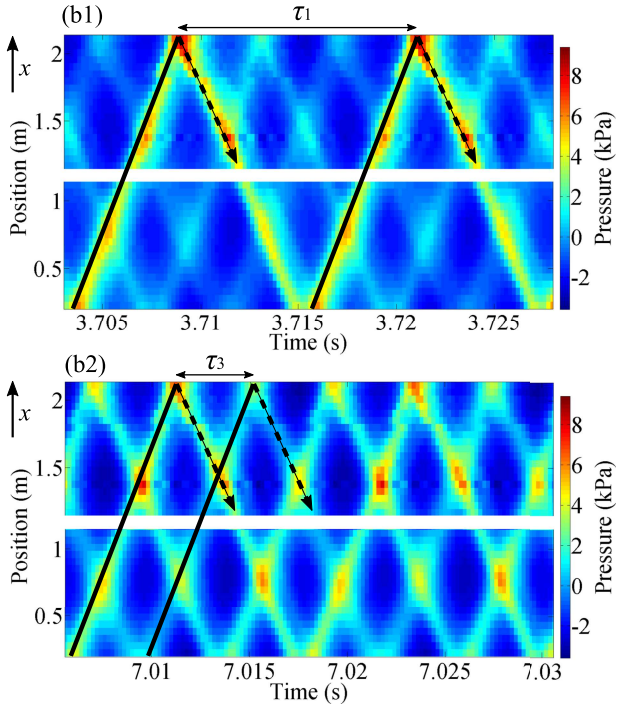

FIG. 6. Spatio-temporal chaotic data obtained from the resonant system at times (b1) and (b2) in Fig. 2(b). Examples of pressure waves propagation in the positive x direction are indicated by solid lines separated by typical time intervals $\tau_1 = 1/f_1$ and $\tau_3 = 1/f_3$. The reflected waves propagating in the negative x direction are indicated by dashed lines. See Multimedia view for a stroboscopic animation corresponding to the first 10 s slow down to 1/3 of the actual speed. Multimedia view: https://doi.org/10.1063/1.5066363.1

time and pressure transducer position, respectively. The color scale represents the gauge pressure measured. The white horizontal bands correspond to the positions of the elbows and connections without pressure transducers. Only a time window of two times the period of the first oscillation mode was used here at the times indicated by (a1), (a2), (b1), and (b2) in Fig. 2.

In Fig. 5(a1), we see six parallel lines separated by one-third of the period of f_1 mode oscillation. In the spatial direction, one can see three wavelengths of approximately a/f_3, which indicates that the spatial pattern is dominated by the f_3 mode. In Fig. 5(a2), the periodicity between the original six pressure waves corresponding to the f_3 mode is broken, while the f_1 mode periodicity is conserved. The pressure waves mostly travel from the hot to the cold side of the stack with much less intense pressure waves going in the negative x direction, just as in other looped thermoacoustic systems showing periodic regimes.[10]

In Fig. 6(b1), for the resonant system, the pressure waves go back and forth with multiple reflections at both ends of the system. Here, the dominant pressure wave is reflected twice in the considered time window, showing that it corresponds to the first mode oscillations, but two less intense intermediate waves corresponding to the third mode oscillations are also visible. In Fig. 6(b2), all pressure wave intensities are roughly similar, showing a dominance of the f_3 mode.

In both systems, the chaotic behavior appears to be governed by underlying f_1 and f_3 mode oscillations in short time scales. In order to study the chaotic dynamics of our systems on longer time lengths, we used the recurrence plot introduced by Eckmann *et al.*[23] This visual tool highlights the times when a trajectory revisits a region of the phase space. It is built from a binary matrix described as

$$\mathbf{R}_{ij} = \Theta\left(\epsilon - \left\|\vec{z}_i - \vec{z}_j\right\|\right), \qquad i,j = 1,\ldots,N, \tag{3}$$

where ϵ is a threshold value. When two points of the phase space $\vec{z}_i$ and $\vec{z}_j$ are closer than a distance ϵ, the states at times i and j are considered to be recurrent and $\mathbf{R}_{ij}$ is equal to 1. On the other hand, if the two points are far from each other, $\mathbf{R}_{ij}$ is equal to 0. By applying this to each point of the attractor, one can obtain a $N \times N$ recurrence matrix with the identity line as an axis of symmetry. By representing the recurrent states with black dots and the others with white dots, various structures appear in recurrent plots:[24] isolated dots occur if the state is not persistent and manifests a random event; diagonal lines parallel to the identity line occur when the trajectory visits the same region of the phase space at different times (the recurrence plot of a perfectly periodic behavior will then contain persistent diagonal lines at intervals corresponding to the period of oscillation); rectangles delimited by horizontal/vertical lines are a sign of almost not changing states for a long time. If the threshold value ϵ is too small, the lack of recurrent points due to noise or a larger sample spacing prevents to learn anything about the recurrence in the system dynamics. If ϵ is too large, distant points of the attractor can be misinterpreted as recurrent states. A threshold value ϵ equal to 10% of the attractor size is commonly considered as the upper limit.[24,25]

Figures 7 and 8 show the recurrence plots obtained from the loop and resonant systems at $T_H/T_C = 2.74 \pm 0.01$ using a long time series of 15 s. The phase space was constructed using the pressure p measured at different positions of the system instead of the embedding method, namely,

$$\vec{z}_i = (p_1, p_2, \ldots, p_M), \tag{4}$$

where M denotes the total number of transducers used. The Euclidean norm was used to determine the threshold value ϵ, which was set to be equal to 10% of the two most distant points in the attractor. ϵ was then of the order of $\sqrt{M}$ times the typical pressure amplitude, with M being the dimension of the phase space, or here the number of used transducers. The bottom figures correspond to the enlarged regions at times (a1), (a2), (b1), and (b2). Only the lower parts of the recurrence plots were computed because of the power limit of our computer.

Figure 7 shows the recurrence plot of the chaotic oscillations in the loop system. Therein, one can see clusters of recurrent points forming kitelike patterns, one of which is labeled ③ in Fig. 7. These patterns are unequally distributed over time, showing that similar phases eventually repeat after some time. The kitelike pattern ③ begins at $t = 5.6$ s, when the third mode oscillations dominate the dynamics as we have already shown in Figs. 2(a1) and 5(a1). In order to make the comparison easier, we have included the spatio-temporal plot of pressure waves in the inset graph of Fig. 7. In the magnified view of the recurrence plot of Fig. 7(a1), however, few intermediate points separated by the period of the third mode $\tau_3 = 1/f_3$ are visible.

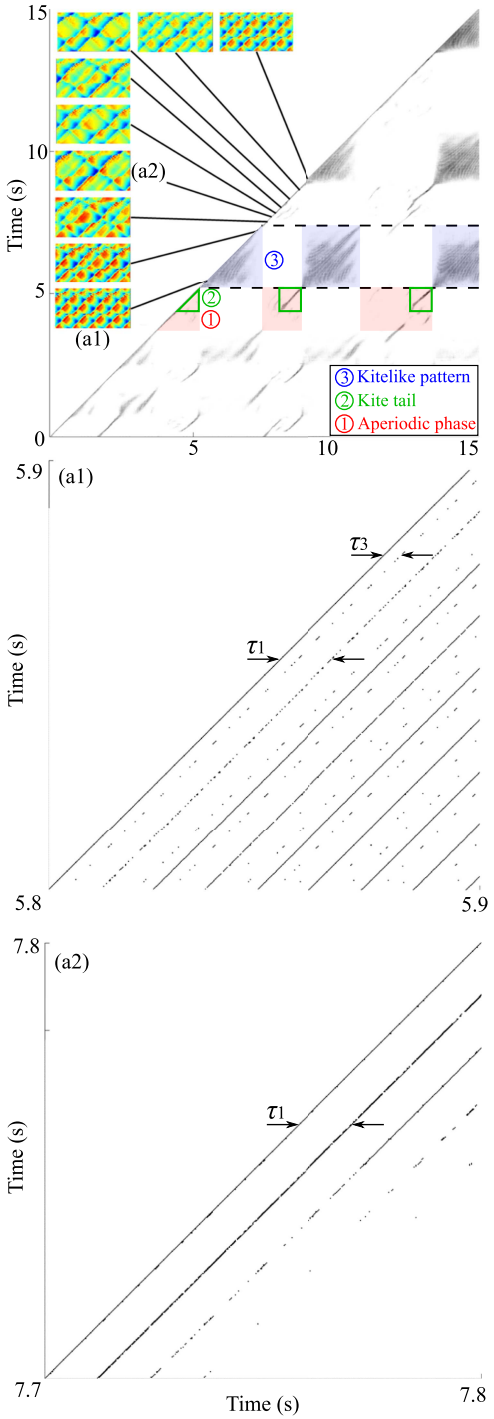

FIG. 7. Recurrence plot of a chaotic behavior observed in the loop system with the spatio-temporal data. Examples of an aperiodic phase, kite tail structure, and kitelike pattern are highlighted in regions ①, ②, and ③ respectively. Bottom figures show the enlarged regions (a1) and (a2) with typical time intervals $\tau_1 = 1/f_1$ and $\tau_3 = 1/f_3$.

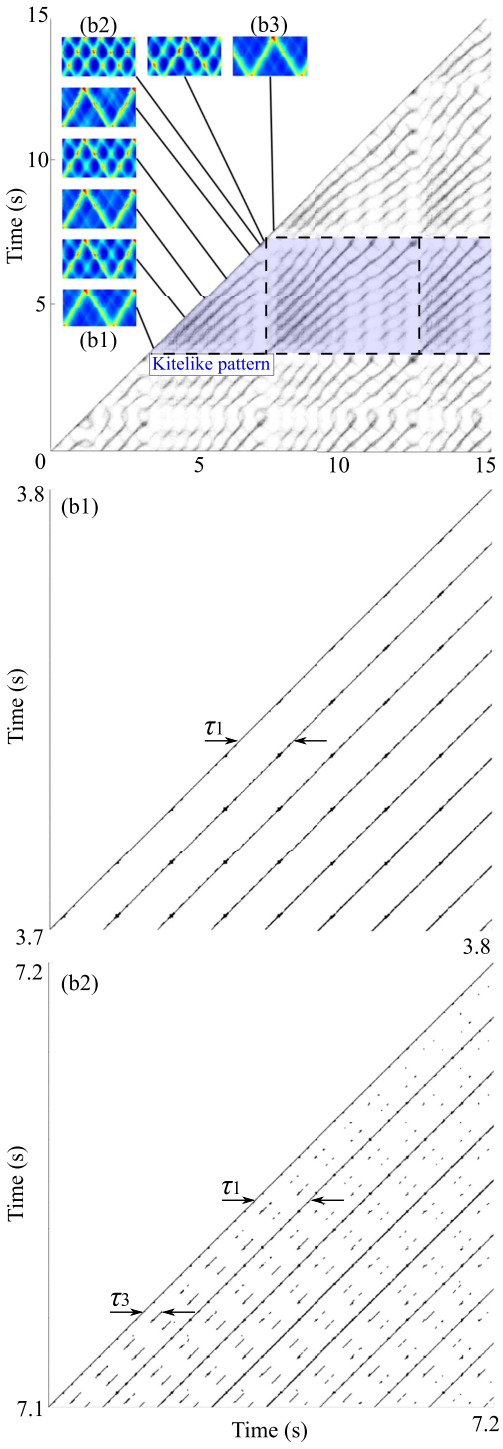

FIG. 8. Recurrence plot of a chaotic behavior observed in the resonance tube with the spatio-temporal data. An example of the kitelike pattern is highlighted between times (b1) and (b2). Bottom figures show the enlarged regions (b1) and (b2) with typical time intervals $\tau_1 = 1/f_1$ and $\tau_3 = 1/f_3$.

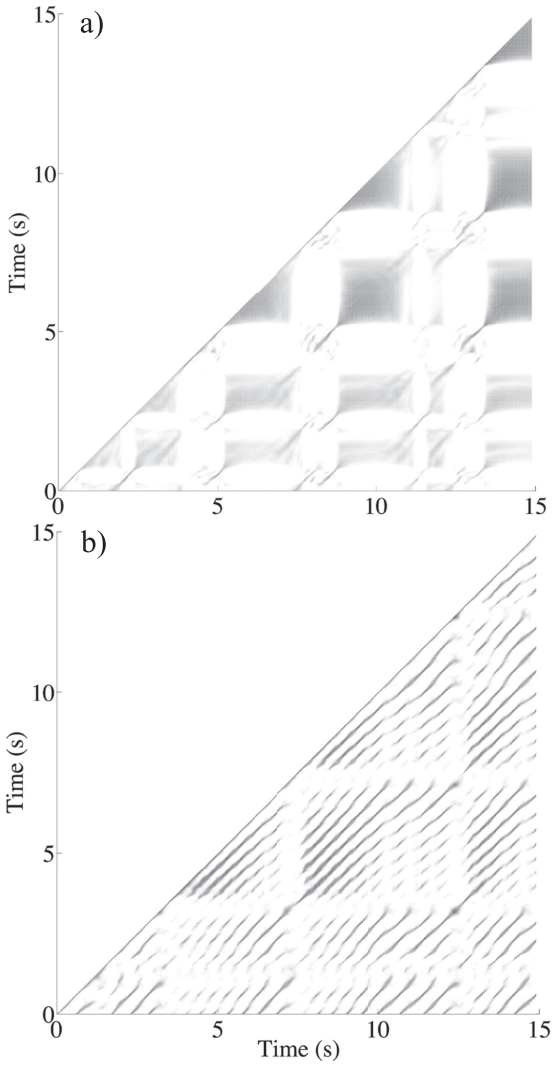

FIG. 9. Recurrence plots of the chaotic behaviors of (a) Fig. 7 and (b) Fig. 8 from a single point measurement at $x = 73$ mm in the looped tube and $x = 2.10$ m in the resonance tube. The phase portraits were build using the embedding method with 8 dimensions.

Instead, we see diagonal lines separated by the first mode oscillations period $\tau_1 = 1/f_1$, indicating that the oscillations are mostly periodic with the fundamental mode oscillations. The absence of solid diagonals for the third mode oscillations results from random fluctuations added by each transducer, which would be overcome by increasing the threshold value ϵ, yet exceeding 10% of the attractor size. In the time interval of (a1), the third mode oscillations are observed, but this mode eventually looses its stability as one can see from the sequence of spatio-temporal plots in Fig. 7. The striped structure at the end of the kitelike patterns originates from a quasiperiodic behavior, i.e., the recurrence in the fast dynamics periodicity is recovered at the period of the beating.[24,26] Aperiodic phases (region ① in Fig. 7) make the transition between each kitelike pattern. During the transition, the first mode oscillations appear with highly fluctuating amplitude, as one can see in the inset graphs starting from (a2). The corresponding enlarged recurrence plot of (a2) shows only a few diagonal lines close to the identity line and separated by the period $\tau_1 = 1/f_1$. At the end of the aperiodic transition, a thin recurrent states cluster forming "tail" of the kitelike pattern is observed (region ② in Fig. 7), showing that this part of the transition is consistently repeated.

In Fig. 8, one can also see kitelike patterns with variable sizes. However, the quasiperiodicity is even more obvious here and the aperiodic transition is absent. The patterns end with curving stripes resulting from changes in the period of the beating, which can be interpreted as underlying frequencies' fluctuations. The spatio-temporal data manifest the mode competition between the first and third oscillation modes. In the enlarged recurrence plot (b1), only the diagonals corresponding to the first oscillation modes are present, while in the enlarged recurrence plot (b2), one can see the short diagonals corresponding to the third mode oscillations starting to appear. During the transition from one pattern to another, the former pressure wave corresponding to the first oscillation mode switches to its first intermediate neighbor to the right as can be seen by comparing the spatio-temporal plots in Figs. 8(b1) and 8(b3).

Though our systems show a quasiperiodic route to chaos, the presence of recurrent patterns in the recurrence plot of the final reachable chaotic states at $T_H/T_C = 2.74 \pm 0.01$ manifests (almost) regular phases that could be a sign of some intermittent phenomena[27,28] as observed by Sujith *et al.* in a combustion system showing type II intermittency.[25] The presence of interrupting chaotic phases is only observed in our loop thermoacoustic system, suggesting some type of intermittency that differs from the chaotic behavior observed in the resonant system.

We also created the recurrence plots by building the phase space with the embedding method using single point measurements and obtained qualitatively similar results, which shows that the chaotic behavior is temporal and not spatio-temporal. Results are shown in Figs. 9(a) and 9(b). Though the multiple-point measurement allowed us to observe wave propagation direction in both thermoacoustic systems, a single point measurement would be sufficient for the recurrence analysis of chaotic oscillations.[29]

IV. SUMMARY

By performing spatio-temporal measurements in a loop and a resonant thermoacoustic oscillator showing chaotic behaviors, we have found that the traveling directions of the pressure waves do not change from those reported in previous studies using periodic thermoacoustic oscillators.

Though the point measurement revealed quasiperiodic routes to chaos with similar correlation dimensions in both systems, the recurrence plots highlighted qualitative differences in the patterns resulting from the mode competition between the modes observed in the routes to chaos. While the chaotic behavior in the loop system consisted of alternations of aperiodic and quasiperiodic phases with increasing beating amplitude, the chaotic behavior in the resonant system showed only quasiperiodic phases with variable durations.

These patterns hint at the existence of different intermittent phenomena or node types in the phase space, which could be investigated

by extracting more information from longer time series such as their lifetime distribution.

ACKNOWLEDGMENTS

This study was financially supported by KAKENHI (No. 26286073).

REFERENCES

[1] G. W. Swift, J. Acoust. Soc. Am. **113**, 2379 (2003).
[2] A. Tominaga, Cryogenics **35**, 427 (1995).
[3] G. W. Swift, J. Acoust. Soc. Am. **84**, 1145 (1988).
[4] T. Yazaki and A. Tominaga, Proc. R. Soc. A **454**, 1471 (1998).
[5] T. Yazaki, A. Iwata, T. Maekawa, and A. Tominaga, Phys. Rev. Lett. **81**, 3128 (1998).
[6] Y. Ueda and C. Kato, J. Acoust. Soc. Am. **124**, 851 (2008).
[7] G. Penelet, V. Gusev, P. Lotton, and M. Bruneau, Phys. Rev. E **72**, 016625 (2005).
[8] T. Biwa, K. Sobata, S. Otake, and T. Yazaki, J. Acoust. Soc. Am. **136**, 965 (2014).
[9] C. Olivier, G. Penelet, G. Poignand, J. Gilbert, and P. Lotton, Acta Acust. United Acust. **101**, 941 (2015).
[10] T. Biwa, T. Takahashi, and T. Yazaki, J. Acoust. Soc. Am. **130**, 3558 (2011).
[11] T. Yazaki, Phys. Rev. E **48**(3), 1806 (1993).
[12] M. Small, D. Yu, and R. G. Harrison, Phys. Rev. Lett. **87**(18), 188101 (2001).
[13] Y. Guan, M. Murugesan, and L. K. B. Li, Chaos **28**, 093109 (2018).
[14] Y. Okuno, M. Small, and H. Gotoda, Chaos **25**, 043107 (2015).
[15] L. Kabiraj, A. Saurabh, P. Wahi, and R. I. Sujith, Chaos **22**, 023129 (2012).
[16] N. Rott, J. Appl. Math. Phys. **20**, 230 (1969).
[17] T. Yazaki, A. Tominaga, and Y. Narahara, J. Low Temp. Phys. **41**, 45 (1980).
[18] A. A. Atchley, H. E. Bass, T. J. Hofler, and H. T. Lin, J. Acoust. Soc. Am. **91**, 734 (1992).
[19] M. Guedra and G. Penelet, Acta Acust. United Acust. **98**, 232 (2012).
[20] H. Hyodo, K. Muraoka, and T. Biwa, J. Phys. Soc. Jpn. **86**, 104401 (2017).
[21] R. Delage, Y. Takayama, and T. Biwa, Chaos **27**, 043111 (2017).
[22] N. H. Packard, J. P. Crutchfield, J. D. Farmer, and R. S. Shaw, Phys. Rev. Lett. **45**(9), 712 (1980).
[23] J. P. Euckmann, S. O. Kamphorts, and R. Ruelle, Europhys. Lett. **4**, 973 (1987).
[24] N. Marwan, M. C. Romano, M. Thiel, and J. Kurths, Phys. Rep. **438**, 237 (2007).
[25] L. Kabiraj and R. I. Sujith, J. Fluid Mech. **713**, 376 (2012).
[26] Y. Zou, M. Thiel, M. C. Romano, P. L. Read, and J. Kurths, Eur. Phys. J. Spec. Top. **164**, 23 (2008).
[27] N. Marwan, N. Wessel, U. Meyerfeldt, A. Schirdewan, and J. Kurths, Phys. Rev. E **66**, 026702 (2002).
[28] K. Klimaszewska and J. J. Żebrowski, Phys. Rev. E **80**, 026214 (2009).
[29] V. Nair, G. Thampi, and R. I. Sujith, J. Fluid Mech. **756**, 470 (2014).